

BRAGG DIFFRACTION TRANSMISSION MICROSCOPY USING HIGHLY MONOCHROMATIC X-RAYS

Stanislav Stoupin^{*1}, Tomasz Kolodziej², Ayman Said², Arthur Campello¹, and Yuri Shvyd'ko²

¹Cornell High Energy Synchrotron Source, Cornell University, Ithaca, NY 14853, USA

²Advanced Photon Source, Argonne National Laboratory, Argonne, IL 60439, USA

^{*}stoupin@cornell.edu

ABSTRACT

Strain field imaging of the crystal lattice of a diamond was performed in Bragg backscattering of highly monochromatic X-rays (photon energy bandwidth $dE \sim 1$ meV) at a photon energy of $E = 23.7$ keV. Quantitative information on the strain distribution was extracted from transmission images generated by scanning the energy of the incident X-rays through the reflectivity curve of a high-indexed diamond Bragg reflection. The use of transmission geometry allowed us to place the area detector close to the sample, preventing geometric blurring of the images. Photon-energy-tunable highly monochromatic X-rays in backscattering combined with sequential topography methods enabled direct mapping of small relative changes (down to 10^{-8}) in the lattice parameter. The obtained micrographs of the strain field can be used for ultra-precise quantitative characterizations of defects in the crystal lattice and possibly the evolution of these defects as functions of external parameters (temperature, pressure, electromagnetic field, etc.).

INTRODUCTION

The analysis of strain fields in crystals using X-ray topography generally requires efforts to decouple the lattice dilation/compression along the studied reflection's reciprocal vector from shear strains representing local tilts of the reflecting atomic planes. These two types of strain result in local deviations from Bragg's law, which can be compensated for by appropriately rotating the crystal. Using a sufficiently monochromatized incident X-ray beam and a sufficiently small angular spread¹, the profiles of the reflected radiation can be analyzed using contour mapping techniques (e.g., Stock et al., 1986) and rocking curve topography (e.g., Lübbert et al., 2000). The dilational and shear strains can be decoupled by adding or subtracting profiles taken at the different angular settings of the reciprocal vector H with respect to the crystal rotation axis or with higher reflection orders (e.g., Stock et al. 1986, Lang et al. 1991, Macrander et al. 2005).

Alternatively, the dilational strain component can be measured selectively at near-exact Bragg backscattering, where the angular acceptance of Bragg's reflections $\Delta\theta$ is maximized ($\Delta\theta \approx 1$ mrad). If θ is the small deviation from normal incidence to the reflecting atomic planes, the differential form of the Bragg's law in backscattering becomes

¹ These should be comparable to the intrinsic angular and energy acceptances of the studied reflection.

This document was presented at the Denver X-ray Conference (DXC) on Applications of X-ray Analysis.

Sponsored by the International Centre for Diffraction Data (ICDD).

This document is provided by ICDD in cooperation with the authors and presenters of the DXC for the express purpose of educating the scientific community.

All copyrights for the document are retained by ICDD.

Usage is restricted for the purposes of education and scientific research.

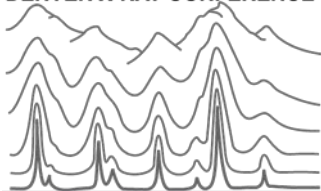
DXC Website

– www.dxcicdd.com

ICDD Website

- www.icdd.com

DENVER X-RAY CONFERENCE®



$$\frac{\delta\lambda}{\lambda} \approx \frac{\delta d}{d} - \Theta\delta\Theta \quad (1)$$

This shows that a small relative change in the incident photon energy $\delta\lambda/\lambda$ probes dilational strain $\delta d/d$ (where d is the interplanar distance) along the reciprocal vector \mathbf{H} ($H=2\pi/d$), while the contribution of angular deviations from shear strain $\delta\Theta$ is suppressed by the factor Θ . A sequence of images of the diffracted X-ray beam profiles taken at different incident X-ray energies across the energy-dependent reflectivity curve of the studied reflection can be used to map dilational strain. High strain sensitivity (up to 1×10^{-8}) can be achieved using photon-energy-tunable X-rays with a photon energy bandwidth ΔE_x comparable to (or less than) the intrinsic bandwidth of the studied reflection ΔE (e.g., Stoupin and Shvyd'ko 2011). In this mode, the crystal's angular coordinates remain fixed, improving the sensitivity of the method.

Better spatial resolution can be attained by using the contrast resulting from the suppression of transmitted radiation. This is done by placing an X-ray area detector at a short distance behind the backscattering crystal. In this case, the projection of the source size to the observation plane is minimized as opposed to the case where one images the reflected beam at the large distances required to obtain necessary separation of the incoming and the reflected beams.

In this paper we present a practical implementation of such a measurement method. The dilational strain of a diamond crystal was mapped in backscattering at a photon energy $E_x = 23.765$ keV using a very-high-resolution monochromator (1-meV-bandwidth). The dilational strain map as well as maps of the crystal reflectivity curve width and peak value were extracted using rocking curve topography methods. This new approach could find a range of applications in areas benefited by the direct, ultra-precise mapping of dilational strain in single crystals. These include the metrology of very-high-resolution X-ray optics, mapping isotopic content in nearly perfect crystals, in-situ microscopy studies of lattice defects, and many others.

EXPERIMENT

The experiment was performed at the 30ID beamline of the Advanced Photon Source, Argonne National Laboratory. The experimental setup is shown on Fig. 1. Synchrotron radiation produced by an undulator X-ray source was pre-monochromatized at a photon energy of 23.765 keV to a bandwidth of about 1 eV using a double-crystal diamond 111 monochromator. A six-bounce Si high-resolution monochromator subsequently monochromatized the beam to a bandwidth of about 1 meV (Toellner et al., 2011). The resulting X-ray beam (meV-beam) was incident on a diamond crystal with (001) surface orientation set to near-backscattering condition of the 3 3 13 reflection (backscattering energy of 23.765 keV at room temperature). The reflected radiation was monitored using an avalanche photodiode (APD) detector. The angular offset from the exact backscattering was $\Theta \approx 1$ mrad. The transmitted X-ray beam was imaged using X-ray area detector microscope with $10\times$ optical magnification (ANDOR NEO, 150- μm -thick scintillator).

The distance from the X-ray source to the diamond crystal was $L_1 \approx 41$ m and the distance from the diamond to the imaging plane of the area detector was $L_2 \approx 10$ cm. The source size was dominated by the APS undulator source size in the horizontal direction $S_h \approx 600 \mu\text{m}$ (FWHM). Therefore, the projection of the source size in the imaging plane was $P_h = S_h L_2/L_1 \approx 1.5 \mu\text{m}$. The spatial resolution in the imaging plane was limited by the point spread function of the scintillator.

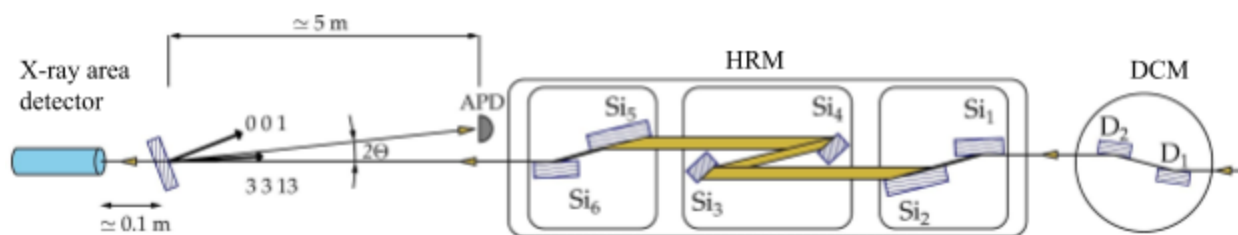


Fig. 1 Experimental setup: Synchrotron radiation produced by is pre-monochromatized using a high-heat load diamond 111 double-crystal monochromator (DCM). A high-resolution six-bounce monochromator (HRM) then monochromatizes the beam to a 1 meV bandwidth. The resulting photon-energy-tunable X-ray beam (meV-beam) is incident on a diamond crystal, which is set to a near-backscattering condition of the 3 3 13 Bragg reflection with a small angular offset $\Theta = 1$ mrad. The reflected radiation is monitored using an avalanche photodiode detector (APD) and the transmitted X-ray beam is imaged using X-ray area detector.

The diamond crystal analyzed was a high-pressure high-temperature grown type IIa 100- μm -thick plate of a trapezoidal shape, (001) surface orientation, and of a very high crystal quality (Stoupin et al., 2013). A sequence of images of the transmitted X-ray beam was taken at different photon energy values on the reflectivity curve of the diamond's 3 3 13 reflection. This sequence was processed using rocking curve topography methods (Stoupin, 2015) to extract transmissivity, curve width and peak position at each pixel across the transmission image of the illuminated crystal. To obtain peak reflectivity an offset was subtracted from the energy-dependent transmissivity curve. The offset was calculated as the transmission level outside of the diffraction region based on the values on the curve's tails. The absolute value of this subtraction normalized by the offset represents the absolute reflectivity of the diamond backscattering reflection (neglecting small absorption of radiation in diamond).

RESULTS AND DISCUSSION

Figure 2(a) shows a conventional white-beam X-ray topograph of the Laue 131 reflection of the diamond plate, which confirms the crystal's high quality. The topograph was recorded on an X-ray film (AGFA STRUCTURIX D3-SC) using bending magnet synchrotron radiation. Bragg diffraction backscattering transmission microscopy was performed for a region located in the corner of the crystal as shown by the dashed box on Fig. 2(a). This region, of size of about $1.0 \times 0.25 \text{ mm}^2$ (limited by the meV beam size) appears defect-free on the white-beam X-ray topograph. This region magnified is also shown on Fig. 2(b). The presence of fine speckle-like features on the crystal reflection as well as outside the reflection suggests that this is noise due to variation in sensitivity of individual emulsion's grains. Bragg diffraction transmission topographs showing maps of peak reflectivity, curve width, and dilational strain along the 3 3 13 direction are shown in Fig. 2(c). The scale of the dilational strain corresponds to the relative change in the photon energy of the monochromator. The incremental change in the photon energy results from the incremental adjustment of angle ψ between the crystal pairs $\text{Si}_{1,2}$ and $\text{Si}_{3,4}$ in the high resolution monochromator (Stoupin and Shvy'dko 2011). The smallest statistically reproducible (in terms of the reflectivity curve centroid position) angular increment is about $\delta\psi \approx 0.1 \mu\text{rad}$. The conversion factor for the change in the photon energy is $\nu \approx 2.83 \text{ meV} / \mu\text{rad}$.

Taking Eq. (1) into account, the precision in the determination of dilational strain can be estimated as $\nu \times \delta\psi/E_x \approx 1 \times 10^{-8}$.

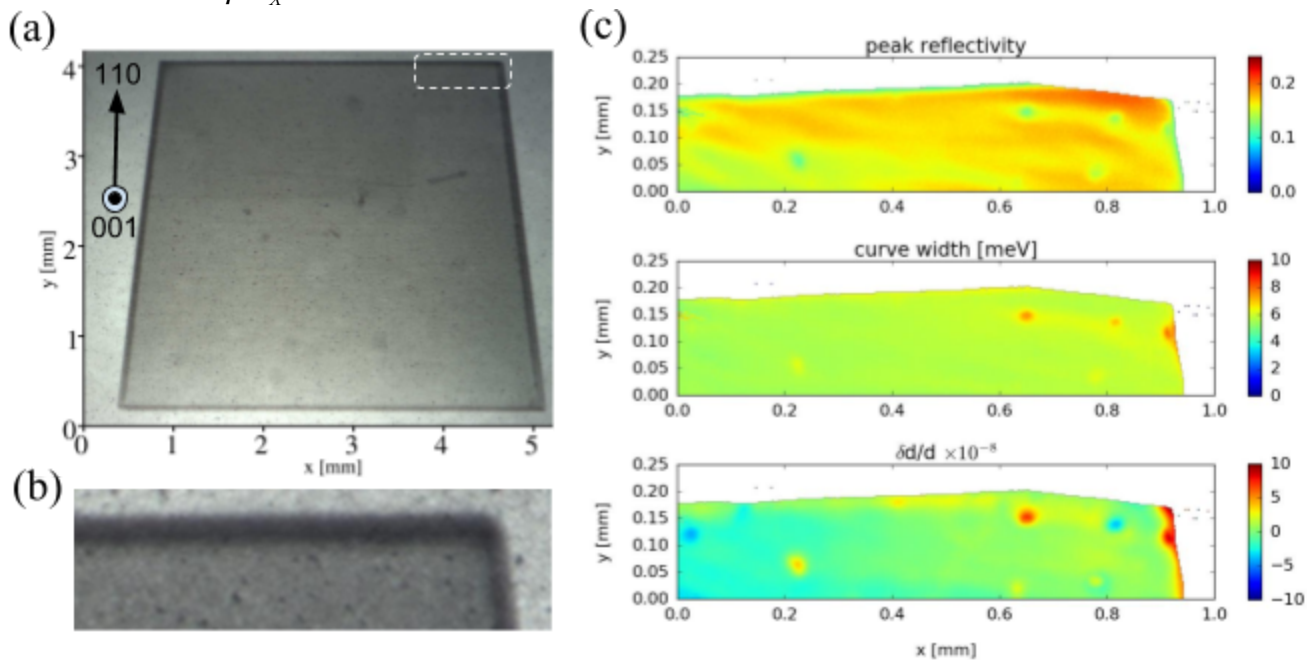


Fig. 2 (a) White beam X-ray topograph (from 131 reflection) of the diamond plate revealing very high crystal quality. The white dashed rectangle shows the region imaged using Bragg diffraction transmission microscopy in backscattering. This region is shown magnified in (b). (c) Bragg diffraction transmission topographs showing maps of peak reflectivity, reflection curve width, and dilational strain.

The Bragg transmission topographs reveal several localized imperfections in the studied region of the crystal that were not resolved by white-beam X-ray topography. For a perfect 100- μm -thick diamond crystal the dynamical theory of diffraction predicts a peak reflectivity of about 0.18 and a reflectivity curve width of about 6 meV (FWHM) in backscattering of the 3 3 13 reflection. Several circular strained regions are observed with diameters of about 20-30 μm . In these regions the reflectivity drops by about factor of 2 and the curve width increases by a few meV. The levels of dilational strain in these regions reach values of about 10^{-7} . For some of these regions, lattice dilation at this level is observed while for others lattice compression is seen. It should be pointed out that these strain fields, although consistent with that of a 3-dimensional defect, do not likely originate from impurities or vacancies of one or a few atoms. Indeed, the strain field of a single substitutional atom in the diamond lattice is expected to be on the order of $6 \times 10^{-5}/r^3$ at a distance r measured in nanometers (e.g., Grazioso et al., 2013). The observation of strain fields originating from atom-sized defects at the 10^{-8} strain sensitivity would require a spatial resolution of about 20 nm, out of the reach of the described experimental setup. Therefore, the observed strain fields could instead result from precipitates/aggregates or voids in the diamond lattice formed during high-pressure high-temperature growth. The precise assignment of these regions to particular types of precipitates would require a more detailed investigation.

SUMMARY

A new method of X-ray diffraction topography was demonstrated where the use of highly monochromatic X-rays in backscattering enabled direct measurements of dilational strain fields in single crystals with a high precision of about 10^{-8} . The method was used to study a selected region in a high-quality 100- μm -thick diamond crystal plate. While no crystal lattice defects were found in this region using traditional white beam X-ray topography, Bragg diffraction transmission topographs revealed several circular strain fields with a maximum level of about 10^{-7} , consistent with those arising from 3-dimensional defects, such as inclusions or voids in the crystal lattice.

In another experiment using the same method, an effect of irradiation with high-flux-density synchrotron beams on the diamond crystal lattice was studied. The high sensitivity to strain in X-ray diffraction imaging was one of the essential tools of the study (Kolodziej et al., 2017).

Besides metrology of very-high-resolution X-ray optics, a variety of other possible applications could be considered. These include studies of micro-mechanical devices made from single crystals, imaging regions of variable isotopic content in single crystals, and imaging studies of thermal expansion in single crystals at low temperatures where relative changes in lattice parameters fall below 10^{-6} .

ACKNOWLEDGEMENTS

J. Kirchmann and K. Goetze are acknowledged for technical support. D. Pagan is acknowledged for helpful discussions. Use of the Advanced Photon Source was supported by the U. S. Department of Energy, Office of Science, under Contract No. DE-AC02-06CH11357.

REFERENCES

Grazioso et al., (2013). “Measurement of the full stress tensor in a crystal using photoluminescence from point defects: The example of nitrogen vacancy centers in diamond” Appl. Phys. Lett. 103, 101905.

Kolodziej et al., (2017). (submitted for publication)

Lang, A.R., Moore, M., Makepeace, A.P.W., Wierzchowski, W., and Welbourn, C.M. (1991). “On the dilatation of synthetic type Ib diamond by substitutional nitrogen impurity” Phil. Trans. R. Soc. Lond. A 337, 497-520.

Lübbert D., Baumbach, T., Härtwig, J., Boller, E. and Pernot, E. (2000). “ μ m-resolved high resolution X-ray diffraction imaging for semiconductor quality control”, Nucl. Instrum. Meth. Phys. Res. B 160, 521 - 527.

Macrander, A.T., Krasnicki, S., Zhong, Y., Maj, J., and Chu, Y. S. et al. (2005). “Strain mapping with parts-per-million resolution in synthetic type-Ib diamond plates” Appl. Phys. Lett. 87, 194113.

Stock, S.R., Chen, H. and Birbaum, H.K. (1986) “The measurement of strain fields by X-ray topographic contour mapping”, Phil. Mag. A 53, 73 - 86.

Stoupin, S. and Shvyd'ko, Yu.V. (2011). “Ultraprecise studies of the thermal expansion coefficient of diamond using backscattering x-ray diffraction”, Phys. Rev. B 83, 104102

Stoupin, S., et al., (2013). “Diamond crystal optics for self-seeding of hard X-rays in X-ray free-electron lasers” , Dia. Rel. Mat. 33, 1-4.

Stoupin, S. (2015). Python-DTXRD, <https://www1.aps.anl.gov/Science/Scientific-Software/DTXRD>

Toellner, T.S. Alatas, A. and Said, A.H. (2011). “Six-reflection meV-monochromator for synchrotron radiation”, J. Synchrotron Rad. 18, 605-611.